

# Thermally managed Z-scan methods investigation of the size-dependent nonlinearity of graphene oxide in various solvents

PAUL BURKINS,<sup>1,3</sup> ROBINSON KUIS,<sup>3</sup> ISAAC BASALDUA,<sup>2,3</sup> ANTHONY M. JOHNSON,<sup>1,2,3,\*</sup>  
SIVA RAM SWAMINATHAN,<sup>4</sup> DAJIE ZHANG,<sup>4</sup> AND SUDHIR TRIVEDI<sup>4</sup>

<sup>1</sup>Department of Physics, University of Maryland Baltimore County, 1000 Hilltop Circle, Baltimore, Maryland 21250, USA

<sup>2</sup>Department of Computer Science and Electrical Engineering, University of Maryland Baltimore County, 1000 Hilltop Circle, Baltimore, Maryland 21250, USA

<sup>3</sup>Center for Advanced Studies in Photonics Research, University of Maryland Baltimore County, 1000 Hilltop Circle, Baltimore, Maryland 21250, USA

<sup>4</sup>Brimrose Corporation of America, 19 Loveton Circle, Sparks, Maryland 21152, USA

\*Corresponding author: amj@umbc.edu

Received 17 August 2016; revised 6 October 2016; accepted 6 October 2016; posted 6 October 2016 (Doc. ID 274009); published 28 October 2016

**Thermally managed Z-scan using a modified chopper was compared to the utilization of a pulse picker with the common calibration material carbon disulfide and then extended to graphene oxide (GO) in different solvents at  $\lambda = 800$  nm. GO in distilled water using femtosecond laser excitation yielded a value of  $(-2.7 \pm .4) \times 10^{-15}$  cm<sup>2</sup>/W for nanometer particles and  $(-1.6 \pm .6) \times 10^{-15}$  cm<sup>2</sup>/W for micrometer-sized particles. Open-aperture Z-scan results using the modified chopper showed no experimental difference.** © 2016 Optical Society of America

**OCIS codes:** (190.0190) Nonlinear optics; (190.4710) Optical nonlinearities in organic materials; (190.7110) Ultrafast nonlinear optics.

<http://dx.doi.org/10.1364/JOSAB.33.002395>

## 1. INTRODUCTION

Nonlinear optics added a valuable tool with the innovation of the Z-scan technique by Sheik-Bahae *et al.* [1]. At its inception, the technique revealed the nonlinear refractive index ( $n_2$ ) resulting from electrostriction, electronic polarization, molecular reorientation, and unwanted thermal effects, as well as the nonlinear absorption coefficient ( $\beta$ ). While these physical mechanisms among others all add to a materials third-order nonlinearity, thermal effects live on a long time scale and contribute the most to the magnitude of  $n_2$ . Analysis of both parts of the complex third-order nonlinearity can be flawed due to thermal effects influence [2]. It has been shown that thermal effects can mask the electronic response, even changing the sign of  $n_2$  [3].

Given that Z-scan is rather simplistic in design, it has been used to characterize numerous materials. One such material of interest is graphene oxide (GO), which has already shown potential for optical limiting applications in the visible and infrared wavelength regions [4]. However, study of these novel materials is often not done at the femtosecond time scale, and not always using low repetition rate laser systems. Thermal effects cannot be avoided, but a measurement can be taken before

they have had a chance to overtake the electronic nonlinear response of the material. An optical setup incorporating a pulse picker or mechanical chopper allows for the experimentalist to alter the amount of pulses hitting a sample per unit time, allowing for the sample to dissipate the heat before the adjacent burst of pulses is affected. The modified chopper gives a longer burst, therefore granting a temporal window large enough to see dynamic changes in the nonlinear refraction and absorption. For instance, if your peak to valley transmittance is changing on the microsecond scale, the signal is most likely dominated by cumulative thermal effects. The pulse picker, with a much faster rise time, reveals the electronic nonlinear properties before heating can take effect, giving a more accurate account of the nonlinearities of the sample.

## 2. EXPERIMENTAL SETUP

The basic Z-scan setup [1] was employed while integrating a pulse picker and a mechanical chopper, using one at a time, to reduce the repetition rate of the laser. A MaiTai (Ti:sapphire, 80 MHz, 130 fs) laser from Spectra Physics was used for its Gaussian spatial TEM<sub>00</sub> mode. First, experiments involving

the modified mechanical chopper were completed. The chopper allowed a burst of pulses through to the sample with complete extinction of the remaining pulses, referred to as the off time. For the experiment a chopper frequency of 150 Hz was used. This gave an off time of 75 ms. The opening rise time had a range of 9–20  $\mu$ s. One detector was used to trigger an oscilloscope by collecting light before hitting the sample. Open-aperture (OA) and closed-aperture (CA) Z-scans were recorded simultaneously using two detectors. The aperture used for CA, attached to the detector, had a 1 mm diameter pinhole, resulting in a relative aperture size  $S = 0.8$ . For this experiment a 10 cm focal length lens was utilized to focus into the 1 mm cell. Note the chopper had a slit 1 mm across and the beam was focused through the slit using a telescope with foci of 7.5 cm.

Next, a Quantum Technology Inc. Pockels cell pulse picker replaced the chopper. This allowed for shorter bursts with a maximum of 80 pulses and a minimum of one pulse when operated in burst mode. Bursts of three pulses and 80 pulses were applied to the sample with similar results. The repetition rate was reduced from 80 MHz to 160 Hz, with an opening rise time of  $\sim 9$  ns. The contrast ratio of extinguished to picked pulses was 250:1. The beam spot size of 25  $\mu$ m was obtained by using a 7.5 cm lens. For both experiments, the laser beam was focused into a 1 mm cell containing 0.5 mg/ml solution of GO dispersed in distilled water. Two mixtures were made, one containing nanometer-sized particles of GO and the other with micrometer-sized particles. A mixture of 0.5 mg/ml of GO in tetrahydrofuran (THF) was also used.

### 3. Z-SCAN THEORY

The Z-scan technique characterizes a material by its reaction to intense laser light. Coherent laser beams generate density changes by way of electronic polarization, electrostriction, molecular reorientation in the case of liquids, and thermal effects. This internal self-action produces a lens in the material which either focuses or defocuses the laser beam. In the far-field this expanding beam can be collected on a detector after traversing a pinhole aperture, referred to as CA Z-scan. Part of the beam exiting the sample can be collected directly by another detector giving OA Z-scan. A transmission profile can be collected as the sample moves through the focus of a focusing lens placed just before the sample. For a positive nonlinearity a typical valley followed by a peak will be seen, and vice versa for a negative nonlinearity in the case of CA Z-scan.

The formalization for Z-scan was outlined by Van Stryland starting with the refractive index [1]. Note that the nonlinear refractive index  $n_2$  below is in electrostatic units (esu), while gamma ( $\gamma$ ), given in some text, is simply the nonlinear refractive index but in meters squared per Watt ( $\text{m}^2/\text{W}$ ):

$$n = n_o + \frac{1}{2}n_2E^2 = n_o + \gamma I. \quad (1)$$

Here  $n_o$  is the linear index of refraction, and  $E^2$  is the square of the electric field. In order to convert from esu to  $\text{m}^2/\text{W}$  one would use the following equation, which includes  $c$ , the speed of light in m/s:

$$n_2(\text{esu}) = \frac{cn_o}{40\pi} \gamma \left( \frac{\text{m}^2}{\text{W}} \right). \quad (2)$$

During the experiment, the on-axis intensity is measured as a function of the sample position. To begin formulating an equation to fit the data one must first decide if the material is considered optically thin. Criterion for thin media is conveyed with the expression  $L \ll z_0$  for linear diffraction and  $L \ll z_0/\Delta\Phi$  for nonlinear refraction, where  $L$  is the thickness of the sample,  $z_0 = \pi\omega_0^2/\lambda$  is the Rayleigh range, with  $\omega_0$  representing the beam waist, and  $\Delta\Phi$  is the on-axis nonlinear phase shift. For linear diffraction it is enough to simplify the expression to  $L < z_0$ , as many values of  $z_0$  were tested by Sheik-Bahae and found that the value for  $n_2$  was unchanged. The second equation is often met because  $\Delta\Phi$  is small, or  $\Delta\Phi < 1$ . The on-axis phase shift at the focus (where  $z = 0$ ) is described as

$$\Delta\Phi(t) = k\Delta n_o(t)L_{\text{eff}}, \quad (3)$$

where  $k = 2\pi/\lambda$  is the wavenumber,  $\Delta n_o = \gamma I_o(t)$ , and  $L_{\text{eff}} = (1 - e^{-\alpha L})/\alpha$ . The intensity at the focus is represented by  $I_o(t)$ . Then  $\alpha$  is the linear absorption coefficient, which is used to calculate the effective length,  $L_{\text{eff}}$ , of the sample, where  $L$  is the thickness of the sample. For thin media, the transmission equation for CA Z-scan can be written in terms of the nonlinear phase shift and the ratio of the sample position to the Rayleigh range:

$$T_{\text{closed}} = 1 + \frac{4x\langle\Delta\Phi\rangle}{(1+x^2)(9+x^2)}; \quad x = \frac{z}{z_0}. \quad (4)$$

This transmission Eq. (4) only applies to CA Z-scan for a Gaussian spatial beam profile. Another comment on the equation is  $\langle\Delta\Phi\rangle$  is the time average of the phase. For Gaussian temporal pulses this is equal to  $\Delta\Phi/\sqrt{2}$  and for hyperbolic secant  $2\Delta\Phi/3$  [5]. A quick check of the phase change can be found using the parameter  $S$ , the aperture linear transmission. For  $|\Delta\Phi| \leq \pi$  the following relation holds:

$$\Delta T_{p-v} \approx 0.406(1-S)^{0.25}|\Delta\Phi|. \quad (5)$$

For OA Z-scan, where the value in question is now the nonlinear absorption, the transmission equation depends on the on axis intensity  $I_o$ , the effective length  $L_{\text{eff}}$ , and the parameter  $x$  defined above. This equation is a summation whose first two terms will be used to fit the data, representing a two-photon absorption process:

$$T_{\text{open}} = \sum_{m=0}^{\infty} \frac{(-q_o)^m}{(m+1)^2}, \quad (6)$$

$$q_o = \frac{(\beta I_o L_{\text{eff}})}{\left(\frac{z}{z_0}\right)^2 + 1}. \quad (7)$$

### 4. THERMAL EFFECTS

Routinely, femtosecond mode-locked lasers [6,7] with high repetition rates have been used for Z-scan experiments. Falconieri [8] points out that because Z-scan is sensitive to local refractive index changes resulting from density fluctuations, thermal effects, which work through the same mechanisms, can dominate. He investigated thermo-optical effects in  $\text{CS}_2$  [9],

remarking that the nonlinearity measurement may be affected by cumulative thermal effects. Gnoli *et al.* [2] claims thermal lensing accumulating over many laser pulses leads to flawed analysis and understanding of the nonlinear response, as well as a shifted origin. Another study showed that pulse duration, not the repetition rate, could also produce variations in the measurement of  $n^2$  [10] as a result of acoustic thermal effects.

The common take on thermal effects (heating) is that they begin and persist with each laser pulse that strikes the sample, with two common contributors, acoustic waves and thermal accumulation and diffusion. The process involves partial absorption of each laser pulse in materials with non-negligible linear absorption or possibly higher-order absorption, where the energy is converted into heat. A temperature gradient is formed due to the shape of the laser beam. This produces a strain that induces acoustic waves that propagate through the sample across the beam diameter, similar to electrostriction. It is believed the time required to see a change in the materials density, resulting in a refractive index change as a consequence of acoustic waves, is referred to as the acoustic transit time ( $t_{\text{acoustic}} = \omega_o/v_s$ ), and is governed by the speed of sound in the material ( $v_s$ ) as well as the size of the beam waist ( $\omega_o$ ) [10]. The same temperature gradient responsible for acoustic waves also generates a thermal lens. This is often referred to as cumulative thermal effects, or thermal diffusion [9], which are thought to become significant at the characteristic time  $t_c$ , [2] which is given by  $t_c = \omega_o^2/4D$ . Here,  $D$  is the thermal diffusivity, which can be found by dividing the thermal conductivity by the materials mass density and specific heat capacity at constant pressure ( $D = \kappa/\rho c_p$ ).

Acoustic waves are more prevalent in the nanosecond and picosecond pulse width regimes. For picosecond pulses, acoustic waves can be induced and experienced by individual pulses. The leading edge of the pulse generates the acoustic wave and the trailing edge feels the effects. In the femtosecond regime, the pulses are in general much shorter than the propagation time, allowing for acoustic waves to be generated but not prevalent enough to affect the same pulse. Although single femtosecond pulses are too short to experience effects from the acoustic wave, the pulse period must be longer than  $t_{\text{acoustic}}$  to allow for adjacent pulses to be affected. The strength of acoustic thermal effects are low in the femtosecond time regime, and are weaker than cumulative effects in general [8]. Specifically, if the acoustic wave has enough time to completely traverse the beam profile, the thermal contribution can be attributed to accumulation of heat within the system.

Cumulative thermal effects are a direct result of the repetition rate. At high repetition rates, the time between pulses is shorter than time  $t_c$ , and the sample does not have enough time to dissipate the heat from the previous pulse out of the beam diameter. This heat continues to build producing a thermal lens, eventually overtaking the electronic and molecular effects, and continuing to very large negative nonlinear refractive indices and high nonlinear absorption.

## 5. SYNTHESIS OF GRAPHENE OXIDE

Graphene oxide was synthesized by the modified Hummers method as described in the literature [11]. First, 200 ml of

a 9:1 vol. mixture of concentrated  $\text{H}_2\text{SO}_4/\text{H}_3\text{PO}_4$  was slowly added to a mixture of 3.0 g of graphite powder and 18.0 g of  $\text{KMnO}_4$  with manual stirring. The reaction slurry was heated at  $50^\circ\text{C}$  for 16 h. Afterward, the reaction slurry was placed in an ice bath and 60 ml of  $\sim 30\%\text{H}_2\text{O}_2$  was slowly added to avoid overheating.

For washing, the as-obtained GO slurry was filtered and washed first with 1:3 vol. conc.  $\text{HCl}/\text{H}_2\text{O}$  followed by distilled water, and finally ethanol. After washing, the wet GO paste was transferred from the filter paper to a Petri dish to dry. The dried GO was dispersed into various solvents for Z-scan measurements.

This is a list of chemicals and materials used to produce the graphene particles: graphite nanopowder (40 nm, MTI Corporation), graphite (C) nanopowder/nanoparticles (C, 400 nm–1.2  $\mu\text{m}$ , 99.9%, natural graphite, hydrophobic, US Research Nanomaterials, Inc), graphite powders (325 mesh, Alfa Aesar, 99.8%, AR), potassium permanganate ( $\text{KMnO}_4$ , 98%, Alfa Aesar), sulfuric acid (ACS, 95.0%–98.0%, Alfa Aesar), phosphoric acid (85% aq. Soln., Alfa Aesar), hydrogen peroxide (ACS, 29%–32% w/w aq. Soln. Alfa Aesar), hydrochloric acid (ACS, 36.5%–38.0%, Alfa Aesar).

## 6. RESULTS AND DISCUSSION

To decrease the chances of misinterpreting the nonlinear response of any sample, actions must be taken to lower the repetition rate of the laser [8], and the beam waist must be designed to match conditions with acoustic and cumulative thermal effects. The beam waist can be changed easily by implementing a beam expander and changing the focusing lens before the sample. The shorter the focus, the faster the acoustic wave will traverse the beam spot. If the acoustic wave is faster than a single pulse or the time between pulses, acoustic contributions can be ignored. The repetition rate, on the other hand, can be changed much easier than the pulse width from the use of a modified chopper or pulse picker. What is an acceptable value for the repetition rate that can minimize the thermal lensing properties? Calculations with the thermal diffusion coefficient for general glasses and liquids yields a characteristic time greater than  $t_c = 40 \mu\text{s}$ , and as a result, the repetition rate should be somewhere in the few tens of kilohertz [8] to match this condition. The repetition rate needs to be on this order to allow general materials time to diffuse heat away from the beam spot, disrupting the construction of a thermal lens. *The chopper rise time is critical in that it must be shorter than the thermal diffusion time, which allows for the data at the rise time to be most representative of the electronic nonlinearity.* Using the mechanical chopper or pulse picker allows for an experimentalist to reduce thermal effects between bursts (sample cools while beam is blocked) and also sheds light on the changes in the nonlinear index and absorption in time.

To demonstrate thermal effects and their influence on the Z-scan technique the common calibration material carbon disulfide,  $\text{CS}_2$ , was examined first with the full repetition rate, and then with an integrated mechanical chopper adopted from Gnoli *et al.* [2] and Falconieri and Salvetti [9]. Measurements taken while operating at the full repetition rate validate the need to lower the repetition rate using a modified chopper

or pulse picker. In the femtosecond pulse width regime the value of  $n_2$  for  $\text{CS}_2$  has been determined to be  $2.1 \times 10^{-15} \text{ cm}^2/\text{W}$  [2], while in Fig. 1(a) a negative nonlinear index of refraction was produced. From this data a fit using the CA transmission equation yields a value of  $n_{2\text{thermal}} = (-1.0 \pm 0.4) \times 10^{-14} \text{ cm}^2/\text{W}$ ; however, thermal effects are not stated to be a nonlinear effect. This data then motivated an investigation to thermally manage the experiment by lowering the repetition rate of the laser. In Fig. 1(b), a CA Z-scan of  $\text{CS}_2$  is shown using the pulse picker. This value was in agreement with the value found in the literature above, prompting measurements with GO.

During the modified chopper experiment the nonlinear refractive index changed from positive to negative of equal magnitude within  $300 \mu\text{s}$  of the opening rise time, shown in Fig. 2(a). Interestingly, for  $\text{CS}_2$  in the case where ultrashort pulses were used to avoid the acoustic wave by focusing tightly, the change in sign of  $n_2$  is similar to the characteristic time. For this experiment the characteristic time was  $104\text{--}134 \mu\text{s}$  depending on the thermal diffusivity used for  $\text{CS}_2$ . It is clear that during the entire burst heat is building within the volume the beam is traversing. This leads to a growing thermal lens, which in turn dominates the nonlinear behavior of the material. In general, the characteristic time does not appear to give a time the nonlinear behavior will change, nor the amount of time required to allow the sample to cool. In Fig. 2(b), you can see the oscilloscope traces obtained in the experiment. For no thermal effects, on the time scale shown, there should be no slope to the central portion of the trace, resembling a square wave. Notice here you can see pre-focus and post-focus traces, and both have a nonzero slope. The black lines at the right are to highlight the change in the end of the burst before and after

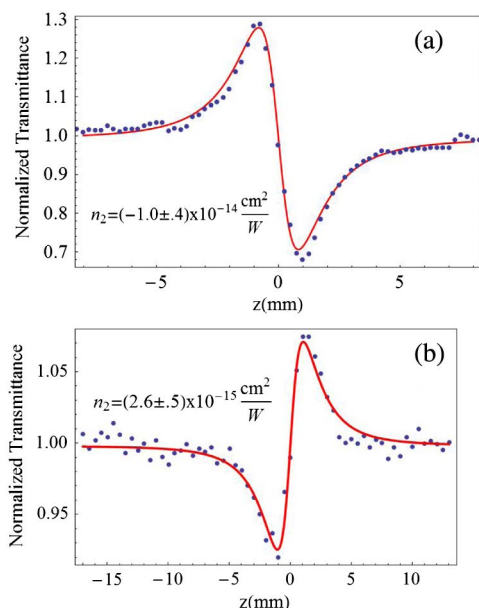


**Fig. 1.** Closed-aperture Z-scan of pure  $\text{CS}_2$  with (a) full (80 MHz) repetition rate, and (b) modified chopper measurements. A negative nonlinear refractive index is derived theoretically from the fit to (a), while  $\text{CS}_2$  is found to be a positive nonlinear material using a pulse picker to reduce heating (b).

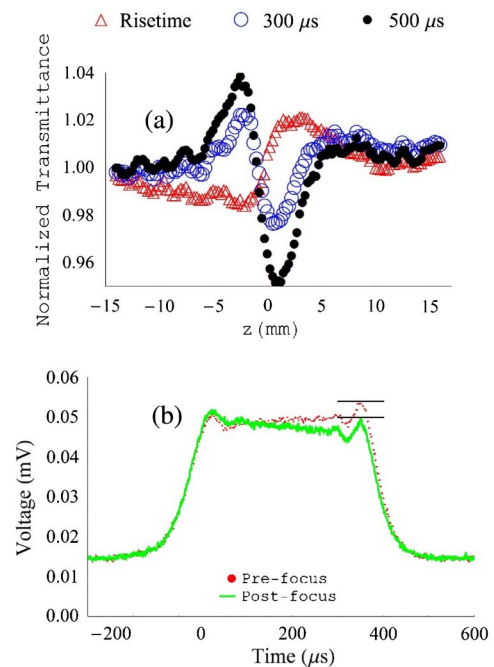


**Fig. 2.** (a)  $\text{CS}_2$  CA Z-scan illustrating the change in the nonlinear refractive index due to heat accumulation in the beam diameter. At different times within the burst. (b) Oscilloscope traces of the burst of pulses collected by the CA detector. The (red) dotted curve is an oscilloscope trace for pre-focus, while the solid (green) represents a post-focus trace. Notice that early in time the pre-focus data is below the post-focus, indicating a positive nonlinearity, while later in the burst (around  $400 \mu\text{s}$ ) the black lines highlight the change in sign of the values.

the focus. Because of this slope the Z-scan trace changes sign. At  $0 \mu\text{s}$  the y-value for the pre-focus trace is less than the post-focus, indicating a positive nonlinear refractive index or a valley followed by a peak. The opposite is true for times beyond  $\sim 100 \mu\text{s}$ .

Once the calibration material showed evidence that thermal contributions could be managed, measurements on GO began. Particularly we started with GO in the solvent THF, where THF seemed to hold the particles in suspension longer than other solvents commonly used. Other studies of GO, predominantly in dimethylformamide (DMF), have been done with nanosecond, picosecond, and femtosecond pulse widths [12,13]. For the 10 cm focus a spot size of approximately  $17 \mu\text{m}$  was obtained. Calculating the acoustic and thermal diffusion times using the speed of sound in THF (1371 m/s) yields 12.4 ns and 0.7 ms, respectively. The repetition rate of the laser produces a pulse every 12.5 ns, so we are just shorter than the acoustic time. This means the acoustic wave should have little effect, although it is already small for femtosecond excitation. The time between bursts is much longer than 0.7 ms, which should allow for any steady-state lens that formed during the burst to relax. It is possible that both the GO and the solvent need to be considered when calculating the thermal times.

Evidence in the CA measurements done with GO in water shows that during the burst the nonlinear index continues to grow in the negative direction, suggesting that thermal contributions increase over the entire burst.

Another stimulating result from GO in water involves the difference in CA Z-scan for different sized particles. The structure and chemical nature of GO can be characterized as flat or folded single- or multi-layer graphite sheets decorated with oxidative ligands including epoxy (R-O-R), hydroxyl (R-OH), and carboxyl (R-COOH) groups, as shown in Fig. 3 [14–17]. The concentrations of these ligand groups are generally higher at the edges of the GO sheets due to the lower coordination number and high degree of defect as compared to the center region. The presence of oxidative ligands and defects in lattice structure at the edges of GO sheets can enhance electron polarization and phonon–phonon scattering leading to increased electronically and thermally induced nonlinear optical effects [18]. The overall optical response of GO under optical irradiation can be divided into two parts: the first is the relative linear response originated from the mostly ordered 2-D GO main lattice. The second part, the nonlinear optical response, is believed to be due to the highly defective lattice at the edges. The volumetric fraction of such defective area increases with reduction in GO size (dimension). Therefore, smaller GO particles may exhibit stronger nonlinear optical properties.

For this study 40 nm and 1.2 μm sized GO particles were dispersed in water using sonification. Again, to see the changes in time, the modified chopper was used. Nanometer GO in water exhibited larger negative nonlinear refraction than its micrometer-sized counterpart for the entire burst, which leads to the conclusion that the nanometer particles dissipate heat slower than the larger particles, seen in Fig. 4. Keep in mind that there will not be a flip in sign here as GO is an electronically negative nonlinear material [12]. This could be a result of there being more nanometer particles in the same volume, causing heat to transfer between particles more readily before it can be dissipated into the solvent, and possibly trapping heat within the beam diameter for longer periods of time. An indicator of this possibility is the non-symmetric nature of the CA Z-scan, symbolic of thermal effects. The electronic nonlinearity may also be higher for the nano-sized particles due to the defects at the lattice edges.

Since the nonlinear refractive index seemed to increase negatively during the entire chopper burst, the value of  $n_2$  with the

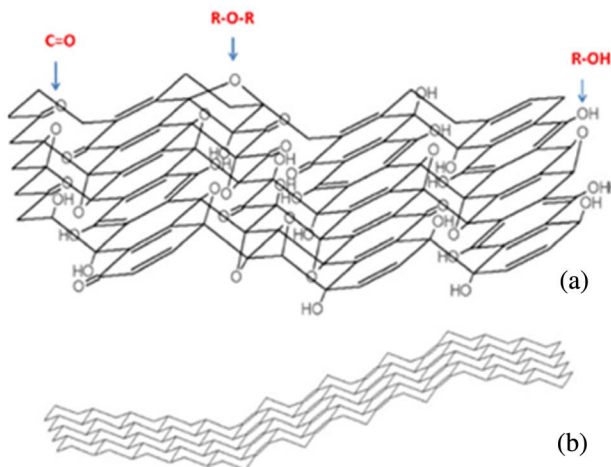


**Fig. 3.** Structure model of GO: (a) surface species and (b) folded carbon skeleton [14].

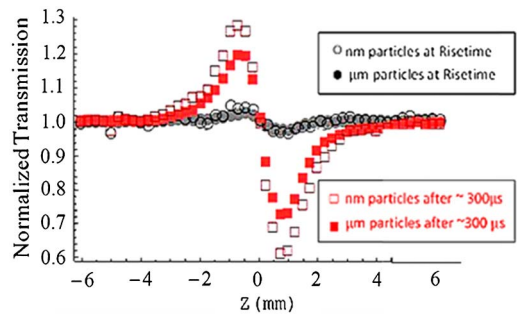


**Fig. 4.** CA Z-scan of GO in distilled water. The nonlinear refraction at the rise time of the burst is represented by circles, while squares represent the fall time. Open shapes are nanometer particles, while closed shapes are micrometer-sized particles. Notice the nanometer particles have a higher nonlinear refractive index at both the rise time and fall time. This also indicates that there are clear thermal effects in the measurement; otherwise the signal should not change on the microsecond time scale.

least thermal contribution was taken from the opening rise time. To verify the value for the nonlinear index, the pulse picker was used to lower the repetition rate to 80 Hz with 80 of the femtosecond pulses per burst. This allowed for a much shorter opening rise time, a much shorter burst, and therefore less time for accumulative thermal effects to increase. Using this setup, it was determined that the nonlinear refractive index for nanometer particles versus micrometer particles differs by approximately  $1.1 \times 10^{-15} \text{ cm}^2/\text{W}$ , shown in Fig. 5.

The values of GO in distilled water are consistent with previous results with GO sheets in DMF giving an  $n_2 = -1.1 \times 10^{-15} \text{ cm}^2/\text{W}$  [12]. It should be noted that the CA data for GO in water was divided by a scan of distilled water. Therefore

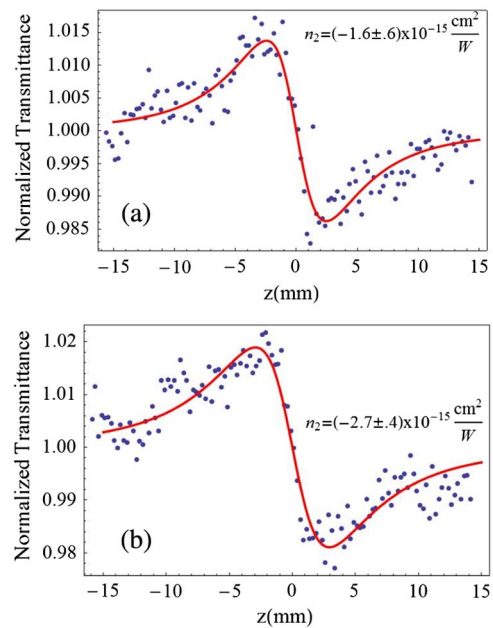


**Fig. 5.** (a) Data and fit of micrometer-sized GO particles in distilled water with a pulse picked 800 nm laser. (b) Data and fit from nanometer-sized GO particles under the same conditions.

this data can be considered the effective nonlinear index of GO particles. The CA scans of GO in THF, pictured in Fig. 6, are an order of magnitude larger than when in water. A possible reason these numbers could be larger is when using the pulse picker the other pulses are not completely extinguished, considering the extinction ratio of 250:1. Each pulse then can add very small amounts of heat to the system at the full repetition rate. These scans were also divided by CA Z-scans of the solvent THF, which showed no nonlinear absorption, but provided a background level.

The chopper measurements of GO in distilled water yielded an average  $n_2$  of  $(-2.6 \pm 1) \times 10^{-15} \text{ cm}^2/\text{W}$  for nanometer particles and  $(-1.8 \pm .8) \times 10^{-15} \text{ cm}^2/\text{W}$  for micrometer-sized particles. Still the nanometer particles have a greater  $n_2$ . These values are taken, however, after approximately 1600 pulses have hit the sample, which means there could be more contributions from thermal effects.

In the femtosecond pulse width regime very high intensities, between 82 and 230  $\text{GW}/\text{cm}^2$ , are required to see the change from saturable absorption to reverse saturable absorption [13], signifying the nonlinear absorption behavior to be intensity-dependent for GO. This experiment, done with just 9.78  $\text{GW}/\text{cm}^2$ , shows that graphene is a saturable absorber at  $\lambda = 800 \text{ nm}$ . This behavior is dependent on the energy levels of GO, and therefore should not change sign due to thermal effects. Just as a word of caution, a scan can appear to do so; however, this phenomenon is an effect of the thermal lens. The beam will enlarge enough to miss the OA detector, producing a decrease in signal or dip. Below in Fig. 7, GO in both solvents are compared using Eq. (6) to fit the data. It appears that while the nonlinear refractive index is dependent on the particle size, the nonlinear absorption is not. In distilled water both

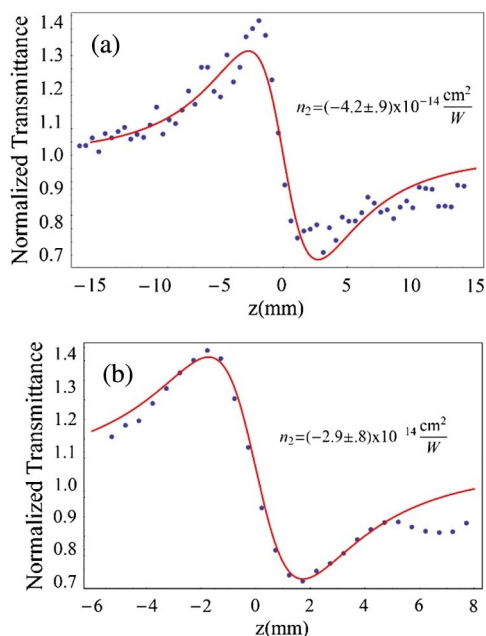


**Fig. 6.** Closed-aperture Z-scan of (a) nm-GO in THF and (b)  $\mu\text{m}$ -GO in THF using the pulse picker. Both sized particles show a negative nonlinearity, with nm-GO showing a larger magnitude nonlinear refractive index.

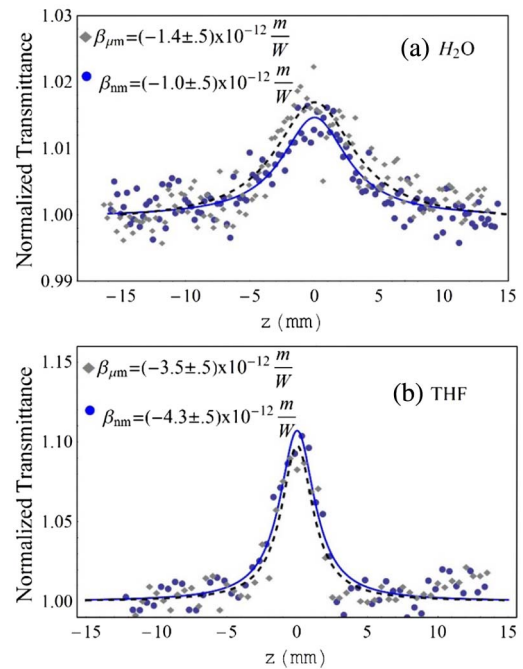


**Fig. 7.** Open-aperture Z-scan taken with the modified chopper at the rise time of the burst where the solution of GO in both (a)  $\text{H}_2\text{O}$  and (b) THF exhibits saturable absorption. It appears the nonlinear absorption of the different sized particles is alike; however, it is smaller in magnitude in  $\text{H}_2\text{O}$ .

particles have a value of  $\beta \sim -1 \times 10^{-12} \text{ m}/\text{W}$  and in THF  $\beta \sim -4 \times 10^{-12} \text{ m}/\text{W}$ .

## 7. CONCLUSION

Thermal effects can contribute and overwhelm nonlinear refractive measurements, as shown in  $\text{CS}_2$ . When the repetition rate is reduced, the pure electronic nonlinearity can be extracted from the experiment. The acoustic and thermal diffusion times that are believed to govern the buildup and relaxation of these effects must be refined. Graphene oxide in different solvents was examined showing small discrepancies between different sized particles in the same solvent, sometimes owing to thermal contributions. Nanometer GO particles seem to have a higher nonlinear refractive index, while their nonlinear absorption is comparable if not the same as the micrometer-sized counterparts. Two methods of controlling thermal effects were used, leading to faster rise times with the pulse picker, but full extinction of the extraneous pulses with the mechanical chopper. If an experiment calls for the most precise value of the electronic nonlinearity then a pulse picker or low rep rate system should be used. If a less expensive option is required or the change in nonlinear properties is important, the mechanical chopper can be used. Another use for the mechanical chopper is to determine if the laser system and setup are yielding data produced from thermal or electronic properties of the material. A change in the sign of  $n_2$ , or a decreasing or increasing signal over time, would indicate that measurements are affected by thermal contributions. For the nonlinear refractive index sometimes a non-symmetric trace is also indicative of thermal effects.

These would not be seen without the use of an oscilloscope, where the Z-scan can be examined in time.

**Acknowledgment.** We would like to thank Eric Van Stryland for talks on thermal properties of materials and their dependence on laser pulse width.

## REFERENCES

1. M. Sheik-Bahae, A. A. Said, and E. W. Van Stryland, "High-sensitivity, single-beam  $n_2$  measurements," *Opt. Lett.* **14**, 955–957 (1989).
2. A. Gnoli, L. Razzari, and M. Righini, "Z-scan measurements using high repetition rate lasers: how to manage thermal effects," *Opt. Express* **13**, 7976–7981 (2005).
3. T. Jian-Guo, W. Hao-Hua, Z. Wen-Yuan, L. Tao, Z. Chun-Ping, and Z. Guang-Yin, "Analysis of the influence of thermal effect on z-scan measurements with a nanosecond pulse laser," *Chin. Phys. Lett.* **17**, 510–512 (2000).
4. N. Liaros, S. Couris, A. Bakandritsos, and A. Kolokithas-Ntoukas, "Broadband optical power limiting of graphene oxide colloids in the picosecond regime," in *15th International Conference on Transparent Optical Networks* (IEEE, 2013).
5. R. L. Sutherland, *Handbook of Nonlinear Optics*, 2nd. (Marcel Dekker, 2003).
6. H. P. Li, C. H. Kam, Y. L. Lam, and W. Ji, "Femtosecond z-scan measurements of nonlinear refraction in nonlinear optical crystals," *Opt. Mater.* **15**, 237–242 (2001).
7. K. Y. Tseng, K. S. Wong, and G. K. L. Wong, "Femtosecond time resolved z-scan investigations of optical nonlinearities in ZnSe," *Opt. Lett.* **21**, 180–182 (1996).
8. M. Falconieri, "Thermo-optical effects in z-scan measurements using high-repetition-rate laser," *J. Opt. A* **1**, 662–667 (1999).
9. M. Falconieri and G. Salvetti, "Simultaneous measurement of pure optical and thermo-optical nonlinearities induced by high-repetition-rate, femtosecond laser pulses: application to CS<sub>2</sub>," *Appl. Phys. B* **69**, 133–136 (1999).
10. R. A. Ganeev, A. I. Rysanyansky, M. Baba, M. Suzuki, N. Ishizawa, M. Turu, S. Sakakibara, and H. Kuroda, "Nonlinear refraction in CS<sub>2</sub>," *Appl. Phys. B* **78**, 433–438 (2004).
11. D. C. Marcano, D. V. Kosynkin, J. M. Berlin, A. Sinitskii, Z. Sun, A. Slesarev, L. B. Alemany, W. Lu, and J. M. Tour, "Improved synthesis of graphene oxide," *ACS Nano* **4**, 4806–4814 (2010).
12. Z. Liu, Y. Wang, X. Zhang, Y. Xu, Y. Chen, and J. Tian, "Nonlinear optical properties of graphene oxide in nanosecond and picosecond regimes," *Appl. Phys. Lett.* **94**, 021902 (2009).
13. X. Zhang, Z. Liu, X. Li, Q. Ma, X. Chen, J. Tian, Y. Xu, and Y. Chen, "Transient thermal effect, nonlinear refraction and nonlinear absorption properties of graphene oxide sheets in dispersion," *Opt. Express* **21**, 7511–7520 (2013).
14. T. Szabo, O. Berkesi, P. Forgo, K. Josepovits, Y. Sanakis, D. Petridis, and I. Dekany, "Evolution of surface functional groups in a series of progressively oxidized graphite oxides," *Chem. Mater.* **18**, 2740–2749 (2006).
15. D. R. Dreyer, S. Park, C. W. Bielawski, and R. S. Ruoff, "The chemistry of graphene oxide," *Chem. Soc. Rev.* **39**, 228–240 (2010).
16. N.-F. Chiu, T.-Y. Huang, and H.-C. Lai, "Graphene oxide based surface plasmon resonance biosensors," in *Advances in Graphene Science*, M. Aliofkhaezai, ed. (InTech, 2013), Chap. 8, p. 280.
17. M. Nasrollahzadeh, F. Babaei, P. Fakhri, and B. Jaleh, "Synthesis, characterization, structural, optical properties and catalytic activity of reduced graphene oxide/copper nanocomposites," *RSC Adv.* **5**, 10782–10789 (2015).
18. X. Mu, X. Wu, T. Zhang, D. B. Go, and T. Luo, "Thermal transport in graphene oxide—from ballistic extreme to amorphous limit," *Sci. Rep.* **4**, 3909 (2014).